Double-layered quantum dots in a magnetic field: The ground state and the far-infrared response

O. Mayrock, S. A. Mikhailov,* T. Darnhofer, and U. Rössler
Institut für Theoretische Physik, Universität Regensburg, D-93040, Regensburg, Germany
(Received 22 May 1997)

We investigate the ground-state properties, the far-infrared (FIR) response, and the collective modes of a square lattice of double-layered quantum dots by applying classical and quantum-mechanical concepts. Using classical self-consistent linear response theory for the dot array we derive analytic results for the magnetoabsorption spectrum and the frequencies, linewidths, and oscillator strengths of the optical and acoustic collective modes including the effect of intercell and intracell interactions. Within the full quantum-mechanical calculation (applying density-functional theory with the local-density approximation) for a single double-layered quantum dot we obtain numerically ground-state properties and the FIR excitation frequencies. We use a quantum dot model with a realistic distribution of background charge, which accounts for surface states and total charge neutrality. In both approaches we study the dependence of the oscillator strengths of the acoustic mode on the asymmetry of the double-layered system in order to give information on the condition for experimental detection. [S0163-1829(97)03848-4]

I. INTRODUCTION

Far-infrared (FIR) response and collective excitations in low-dimensional electron systems (ES) have been intensively studied, both theoretically and experimentally, during the past two decades. Magnetoplasma excitations have been observed in single-layered two-dimensional (2D) ES in Si metal-oxide-semiconductor field-effect transistors and in $GaAs/Al_xGa_{1-x}As$ heterostructures,[1] in one-dimensional (1D) ES in quantum-wire structures (for reviews see, e.g., Refs. 2 and 3) and in zero-dimensional ES in quantum-dot structures.[4]

In multilayered low-dimensional ES the higher number of degrees of freedom gives rise to additional modes. In double-layered structures one has, besides an optical mode, with in-phase motion of the charge density in both layers (which corresponds to the single dot mode), as an additional feature an acoustic mode with out-of-phase motion. Optical and acoustic magnetoplasma modes have been observed in double-layered 2D systems[5,6] (using Raman scattering) and in double-layered quantum wire arrays[7–9] (using FIR transmission technique). In recent FIR transmission experiments[10] with an array of double-layered dots observation of an acoustic mode has been mentioned. Theoretically, the problem of plasma oscillations in double-layered quantum wires has been considered in Refs. 11–13.

The main problem in detecting the acoustic mode in the FIR spectrum of double-layered systems is its small oscillator strength. It differs from zero only in the asymmetric case (when upper and lower system are not identical) and its value depends on the system parameters. Theoretical studies can be helpful to find the conditions for the observability of the acoustic modes.

In this paper we investigate the FIR response and collective modes of a square lattice of double-layered quantum dots. In Sec. II the problem is studied within the classical self-consistent linear response approach. We calculate analytically the magnetoabsorption and excitation spectra of the system, the dependencies of the linewidths and oscillator strengths of the collective modes on magnetic field, and other parameters of the structure. An influence of the intercell interaction on the excitation spectrum is discussed. In Sec. III we perform full quantum-mechanical calculations within density-functional theory in the local-density approximation of the ground-state properties and the FIR excitation frequencies of a single double-layered quantum dot in the random-phase approximation (RPA) formalism. This approach has been extensively used for calculations of the properties of single-layered dots with electrons and holes.[14–18] Our quantum-mechanical model of the dot includes a realistic distribution of a background charge, which accounts for surface states and *total* charge neutrality. We discuss the differences in the results from classical and quantum-mechanical calculations and study the oscillator strength of the acoustic mode in order to give information on the condition for its experimental detection. In Sec. IV we make conclusions and compare our results with the experimental data of Ref. 10. Throughout the paper we use the effective-mass approximation and neglect spin effects. 2D layers are assumed to be infinitely thin, and the tunneling of electrons between the dots is neglected.

II. CLASSICAL APPROACH

A. Qualitative consideration

Before starting the discussion of an analytic quantitative model we briefly outline the qualitative features of the structure. The double-layered quantum-dot system can be considered as two disks with the radii R_1 and R_2, and 2D equilibrium charge densities $n_{s,1}$ and $n_{s,2}$ separated by a distance D in the z (or growth) direction. The negative charge of electrons in dots is assumed to be compensated by a neutralizing positive background with the same shape. Charge-density plasma oscillations in the system arise when the mobile elec-

trons in the discs are displaced in a lateral direction by x_j relative to the positive background. The restoring force which acts on electrons of the jth layer consists of two contributions. The first contribution is due to the charge density fluctuation in the same (jth) layer. It depends on $n_{s,j}$ and R_j, and is proportional to the displacement x_j. In the absence of the second layer this restoring force results in single-dot plasma oscillations with a frequency $\omega_0 \propto (n_{s,j}/R_j)^{1/2}$. The second contribution is due to the charge-density fluctuations in the other (kth, $k \neq j$) layer. It depends on $n_{s,k}$, R_k, and x_k, as well as on the distance between the dots D. This contribution decreases as $1/D^3$ when $D \to \infty$ due to the dipole force between the layers. The double-layered quantum-dot structure is thus a system of two coupled harmonic oscillators and maintains two types of oscillations. In a symmetric system ($n_{s,1}=n_{s,2}$, $R_1=R_2$) the high-frequency (optical) mode corresponds to in-phase oscillations, the low-frequency (acoustic) mode—to out-of-phase oscillations of the charge in the two layers. In the limit of small D the frequency of the optical mode increases by a factor of $\sqrt{2}$ over that of a single dot, due to a doubling of the restoring force in two layers. The frequency of the acoustic mode tends to zero because of the total compensation of the Coulomb restoring force in a symmetric system in the limit $D \to 0$.

This simple classical picture gives the general description of the plasma oscillations in the system, but does not describe some peculiarities of the excitation spectrum that arise in a quantum-mechanical treatment of the problem. These new features will be discussed in detail in Sec. III.

B. Formalism

The periodic array of double-layered quantum dots is modeled[19] by assuming an equilibrium electron density of 2D electrons $N_0(\mathbf{r},z)=N_1^0(\mathbf{r})\,\delta(z-z_1)+N_2^0(\mathbf{r})\,\delta(z-z_2)$ which is a periodic function of $\mathbf{r}=(x,y)$,

$$N_j^0(\mathbf{r})=\sum_{k,l} n_j^0(\mathbf{r}-\mathbf{a}_{k,l})=\sum_{\mathbf{G}} N_{j,\mathbf{G}}^0 e^{i\mathbf{G}\cdot\mathbf{r}}. \tag{1}$$

The functions $n_j^0(\mathbf{r}) \equiv n_j^0(r)$, $j=1,2$ describe a density profile inside the dots in the planes $z=z_1$ and $z=z_2$;

$$N_{j,\mathbf{G}}^0=\frac{1}{a^2}\int_{\text{cell}} n_j^0(\mathbf{r})e^{-i\mathbf{G}\cdot\mathbf{r}}d\mathbf{r} \equiv \langle n_j^0(\mathbf{r})e^{-i\mathbf{G}\cdot\mathbf{r}}\rangle \tag{2}$$

are Fourier components of $N_j^0(\mathbf{r})$, $\mathbf{a}_{k,l}=a(k,l)$ and $\mathbf{G}_{m,n}=(2\pi/a)(m,n)$ are the lattice and reciprocal lattice vectors respectively, a is the lattice period, and the angular brackets mean the average over an elementary cell. The background dielectric constant ϵ is assumed to be uniform in all the space and the structure is placed in a perpendicular magnetic field $\mathbf{B}=(0,0,B)$. The electric field of an external electromagnetic wave, $E_\alpha^{\text{ext}} \propto \exp(-i\omega t)$, $\alpha=\{x,y\}$, is assumed to be uniform and parallel to the plane $z=0$. Both the lattice constant a and the distance between the dots $D=|z_2-z_1|$ are assumed to be small as compared with the wavelength of light $\lambda=2\pi c/\omega\sqrt{\epsilon}$, c is the velocity of light.

An incident electromagnetic wave results in fluctuations of the charge density and the induced potential, which are related by the Poisson equation (quasistatic approximation)

$$\Delta\varphi_{\text{ind}}=-4\pi\{\rho_1\delta(z-z_1)+\rho_2\delta(z-z_2)\}/\epsilon. \tag{3}$$

Expanding all quantities in Fourier series we obtain relations between the Fourier components of the induced electric field and the induced charge densities in the planes $z=z_j$, $j=1,2$,

$$E_\alpha^{\text{ind}}(\mathbf{r},z_j)=-\sum_{\mathbf{G}\neq\mathbf{0}} \frac{2\pi i G_\alpha}{\epsilon G}\sum_{k=1}^{2}\rho_{k,\mathbf{G}}e^{i\mathbf{G}\cdot\mathbf{r}-G|z_j-z_k|}, \tag{4}$$

where $G=|\mathbf{G}|$. The relation between the charge density fluctuations $\rho_{j,\mathbf{G}}$ and the total electric field $E_\alpha^{\text{tot}}(\mathbf{r},z_j)=E_\alpha^{\text{ind}}(\mathbf{r},z_j)+E_\alpha^{\text{ext}}(z_j)$ inside the dots can be found from the continuity equation and the local Ohm's law,

$$\rho_{j,\mathbf{G}}=G_\alpha\langle\sigma_{\alpha\beta}^{(j)}(\mathbf{r})E_\beta^{\text{tot}}(\mathbf{r},z_j)e^{-i\mathbf{G}\cdot\mathbf{r}}\rangle/\omega. \tag{5}$$

Here $\sigma_{\alpha\beta}^{(j)}(\omega,\mathbf{r})$ is the frequency and magnetic-field-dependent conductivity tensor assumed to be proportional to the local electron density $n_j^0(\mathbf{r})$ in a dot of the jth layer. The validity of the local Ohm's law implies that the value v_F/ω (v_F/ω_c in a strong magnetic field) is small as compared with the typical scale of changing the electric field inside the dots (here ω_c is the cyclotron frequency and v_F is the Fermi velocity of electrons in the dots).

Substituting Eq. (5) into Eqs. (4), we obtain a system of coupled integral equations for the induced electric field inside the dots. This system is solved approximately by the method proposed in Ref. 19. Assuming that the induced (and total) electric field *inside the dots* is uniform (consistent with assuming the local Ohm's law), multiplying the first of the Eqs. (4) by $n_1^0(\mathbf{r})$ and the second one by $n_2^0(\mathbf{r})$ and integrating over the elementary cell, we obtain relations between the total electric fields inside the dots $E_\pm^{\text{tot}}(z_j)$ and the external field $E_\pm^{\text{ext}}$,

$$\zeta_{1,1}^{\pm}(\omega)E_\pm^{\text{tot}}(z_1)+\zeta_{1,2}^{\pm}(\omega)E_\pm^{\text{tot}}(z_2)=E_\pm^{\text{ext}}, \tag{6}$$

$$\zeta_{2,1}^{\pm}(\omega)E_\pm^{\text{tot}}(z_1)+\zeta_{2,2}^{\pm}(\omega)E_\pm^{\text{tot}}(z_2)=E_\pm^{\text{ext}}. \tag{7}$$

For the square lattice of circular dots these relations can be written in terms of the $\pm$ circular components of the electric field $E_\pm=(E_x \mp iE_y)/\sqrt{2}$, where the upper sign corresponds to the polarization of the cyclotron resonance of electrons; as $D \ll \lambda$, we have $E_\pm^{\text{ext}}(z_1) \approx E_\pm^{\text{ext}}(z_2) \approx E_\pm^{\text{ext}}$. The functions $\zeta_{j,k}^{\pm}$ in Eqs. (6) and (7) are defined as

$$\zeta_{j,k}^{\pm}(\omega)=\delta_{j,k}+\frac{\pi i\langle\sigma_\pm^{(k)}\rangle}{\omega\epsilon}\sum_{\mathbf{G}\neq\mathbf{0}} G\beta_j(G)\beta_k^*(G)e^{-G|z_j-z_k|}, \tag{8}$$

where $\sigma_\pm=\sigma_{xx}\pm i\sigma_{xy}$. The form factors $\beta_j(G)$ are determined by the Fourier components of the equilibrium electron densities in the dots,

$$\beta_j(G)=\frac{\langle n_j^0(\mathbf{r})e^{i\mathbf{G}\cdot\mathbf{r}}\rangle}{\langle n_j^0(\mathbf{r})\rangle}; \tag{9}$$

$\beta_k^*(G)$ means the complex conjugate, for circular dots $\beta_j(G)$ are real. Equation (8) generalizes the definition (Ref. 19) of the response function of the single-layered dot lattice.

Using Eqs. (6) and (7) we find the total electric field inside the dots, as well as the macroscopic conductivity de-

fined as $\sigma_{\pm}^{\rm macro}=(\langle j_{\pm}^{(1)}\rangle+\langle j_{\pm}^{(2)}\rangle)/E_{\pm}^{\rm ext}$. The absorption coefficient $\Lambda_{\pm}(\omega)$ is then determined by the real part of $\sigma_{\pm}^{\rm macro}$, so that we have

$$\Lambda_{\pm}(\omega)={\rm Re}\left[\frac{\langle\sigma_{\pm}^{(1)}\rangle(\zeta_{2,2}^{\pm}-\zeta_{1,2}^{\pm})+\langle\sigma_{\pm}^{(2)}\rangle(\zeta_{1,1}^{\pm}-\zeta_{2,1}^{\pm})}{\zeta_{1,1}^{\pm}\zeta_{2,2}^{\pm}-\zeta_{1,2}^{\pm}\zeta_{2,1}^{\pm}}\right]. \tag{10}$$

The spectrum of collective excitations is determined by zeros of the denominator of Eq. (10),

$$\zeta_{1,1}^{\pm}(\omega)\zeta_{2,2}^{\pm}(\omega)-\zeta_{1,2}^{\pm}(\omega)\zeta_{2,1}^{\pm}(\omega)=0. \tag{11}$$

Using the Drude expressions for the conductivity in the presence of a magnetic field, $\langle\sigma_{\pm}^{(j)}\rangle=if_jn_{s,j}e^2/[m_j^*(\omega\mp\omega_{c,j}+i\gamma_j)]$, we rewrite Eq. (8) for ζ functions in the form

$$\zeta_{j,k}^{\pm}(\omega)=\delta_{j,k}-\frac{\Omega_{j,k}^2}{\omega(\omega\mp\omega_{c,k}+i\gamma_k)}, \tag{12}$$

where e, m_j^*, and γ_j are the charge, effective mass and momentum relaxation rate of electrons in the jth layer, respectively, $\omega_{c,j}=eB/m_j^*c$ is the cyclotron frequency, and

$$\Omega_{j,k}^2=\frac{\pi\langle n_k^0(\mathbf{r})\rangle e^2}{m_k^*\epsilon}\sum_{\mathbf{G}\neq\mathbf{0}}G\beta_j(G)\beta_k^*(G)e^{-G|z_j-z_k|}. \tag{13}$$

The average density over the cell $\langle n_j^0(\mathbf{r})\rangle$ can be written as $\langle n_j^0(\mathbf{r})\rangle=f_jn_{s,j}$, where $n_{s,j}$ is the average carrier density in the dots, and $f_j=\pi R_j^2/a^2$ is the area filling factor. Equations (8)–(13) provide a functional dependence of the absorption and excitation spectra of the system on the equilibrium electron density and other physical and geometrical parameters of the structure.

C. Analysis of results

1. Absorption and excitation spectra: Optical and acoustic modes

Figure 1 exhibits magnetic-field-dependent absorption spectra (a) and collective mode frequencies (b) of the double-layered quantum-dot structure at different electron densities $n_{s,1}$ and $n_{s,2}$ in two layers. The spectrum consists of two, optical and acoustic, modes for each ($\pm$) circular polarization. If the cyclotron masses of electrons in different layers are the same (but other parameters, e.g., electron densities or radii, are different) the dispersion relation, Eq. (11) gives the following expressions for the frequencies of the $\pm$ polarized optical and acoustic modes of the structure at $\omega_{\pm}^{\rm opt,ac}\gg\gamma_j$:

$$\omega_{\pm}^{\rm opt,ac}=\pm\omega_c/2+\sqrt{(\omega_c/2)^2+\Omega_{\rm opt,ac}^2}, \tag{14}$$

where

$$\Omega_{\rm opt,ac}^2=\frac{\Omega_{1,1}^2+\Omega_{2,2}^2}{2}\pm\sqrt{\left(\frac{\Omega_{1,1}^2-\Omega_{2,2}^2}{2}\right)^2+\Omega_{1,2}^2\Omega_{2,1}^2}. \tag{15}$$

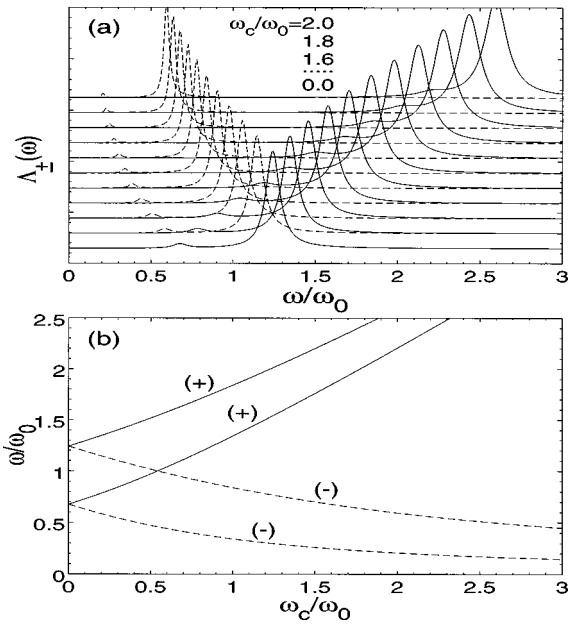

FIG. 1. Magnetic field dependence of (a) the absorption spectrum and (b) the frequencies of the optical (upper curves) and acoustic (lower curves) $+$ (solid curves) and $-$ (dashed curves) polarized excitation modes in a double-layered quantum-dot structure. Effective masses of electrons in the dots, as well as the dot radii are assumed to be identical; the average area densities of electrons in the dots are $n_{s,1}$ and $n_{s,2}$. The frequency ω_0 is defined as $\omega_0^2=3\pi^2(n_{s,1}+n_{s,2})e^2/8m^*\epsilon R$, the density asymmetry parameter α is $\alpha\equiv(n_{s,1}-n_{s,2})/(n_{s,1}+n_{s,2})=0.4$. The intracell interaction parameter is $\Delta_{\rm intra}=0.4$, $\gamma/\omega_0=0.1$.

The upper (lower) sign in Eq. (15) corresponds to the optical (acoustic) mode. For identical dots, we have $\Omega_{1,1}^2=\Omega_{2,2}^2$, $\Omega_{1,2}^2=\Omega_{2,1}^2$, and the frequencies $\Omega_{\rm opt,ac}$ assume the simple form

$$\Omega_{\rm opt,ac}^2=\frac{\pi fn_se^2}{m^*\epsilon}\sum_{\mathbf{G}\neq\mathbf{0}}G|\beta(G)|^2(1\pm e^{-GD}). \tag{16}$$

2. Intercell interaction

Equations (15) and (16) take into account an interaction of plasma modes in different dots both within *the same* elementary cell (*intracell* interaction) and in *different* elementary cells (*intercell* interaction). The intercell interaction is relatively small and can be estimated as follows. Applying the transformation

$$\sum_{\mathbf{G}}F(\mathbf{G})=\int\frac{a^2d\mathbf{q}}{(2\pi)^2}F(\mathbf{q})\sum_{l,m}e^{i\mathbf{q}\mathbf{a}_{l,m}} \tag{17}$$

to Eq. (16) (we restrict ourselves to the symmetric case now) we obtain

$$\Omega_{\rm opt,ac}^2=\frac{\pi n_se^2R^2}{2m^*\epsilon}\sum_{l,m}\int_0^\infty q^2dq(1\pm e^{-qD})|\beta(q)|^2J_0(qa_{l,m}), \tag{18}$$

where $a_{l,m}=a\sqrt{l^2+m^2}$. The term of the sum with $l=m=0$ does not depend on a and describes the frequencies of modes in a single cell. All other terms of the sum (with l^2+m^2

$\neq 0$) give corrections due to the inter-cell interaction. Assuming for simplicity that the density profiles in the dots are given by

$$n_1^0(r) = n_2^0(r) = \tfrac{3}{2} n_s (1 - r^2/R^2)^{1/2} \tag{19}$$

(an oblate spheroid model[20,21]) we obtain $\beta(G) = (9\pi/2)^{1/2} J_{3/2}(GR)/(GR)^{3/2}$, and

$$\Omega^2_{\rm opt,ac} = \omega_0^2 \{ 1 \pm \Delta_{\rm intra} - \Delta^{\rm opt,ac}_{\rm inter} \}. \tag{20}$$

Here ω_0 is the frequency of the dipole plasma mode in a single dot at $B=0$, $\omega_0^2 = 3\pi^2 n_s e^2/4m^*\epsilon R$.[20,21] For $R,\ D \ll a$ the intercell interaction can be expressed by

$$\Delta^{\rm opt}_{\rm inter} = \frac{4\eta(3/2)}{3\pi} \frac{R^3}{a^3}, \quad \Delta^{\rm ac}_{\rm inter} = \frac{3\eta(5/2)}{\pi} \frac{R^3 D^2}{a^5}, \tag{21}$$

where $\eta(z) = \Sigma (l^2 + m^2)^{-z}$ (the sum is taken over all l,m excluding $l = m = 0$); $\eta(3/2) = 9.03$, $\eta(5/2) = 5.09$. $\Delta^{\rm opt}_{\rm inter}$ agrees with that obtained for a single-dot array.[22,23,19] For the acoustic mode the intercell correction has an additional small factor $\sim D^2/a^2 \ll 1$ compared to the optical mode. This is because the dipole moment of the acoustic mode in a symmetric double-layered dot structure is zero, and the intercell interaction is due to higher multipole moments.

The intercell interaction in typical single-layered structures does not usually exceed several percents.[23] This is equally valid for the optical modes in double-layered quantum-dot structures. For the acoustic modes the intercell interaction is even smaller. We neglect below the terms responsible for the intercell interaction and consider only a single cell of a double-layered quantum-dot structure.

It should be noted that the intercell interaction leads to another type of ''acoustic'' modes in an array of double-layered (as well as of single-layered) quantum dots. These modes correspond to out-of-phase oscillations of an electron density in *adjacent* dots within the same layer, and are characterized by a finite lateral quasi-wave-vector q. We do not consider these modes here as due to inequality $a \ll \lambda$ they cannot be seen in FIR experiments.

3. Intracell interaction

The intracell interaction of modes $\Delta_{\rm intra}$ in Eq. (20) is a function of D/R. For the dots with the density profile of Eq. (19) it has the form

$$\Delta_{\rm intra}(z) = 3 \int_0^\infty \frac{dx}{x} J^2_{3/2}(x) e^{-xz}, \quad z = D/R, \tag{22}$$

with $\Delta_{\rm intra}(z \gg 1) \approx 4/3\pi z^3$ and $\Delta_{\rm intra}(z \ll 1) \approx 1 - (3z/\pi)\ln(2/z)$. Figure 2 shows the dependence of the frequencies, Eq. (20), on the ratio D/R in a single cell ($a \to \infty$). When $D \to \infty$ the intracell interaction parameter $\Delta_{\rm intra}$ tends to zero as $1/D^3$, which reflects the dipole character of the Coulomb interaction between the modes in the dots within an elementary cell. When D tends to zero, the frequency of the optical mode increases, as compared to a limit of decoupled dots, by a factor of $\sqrt{2}$. The frequency of the acoustic mode vanishes in the limit $D \to 0$. This result agrees with classical calculations for a double-layered quantum-wire structure,[12]

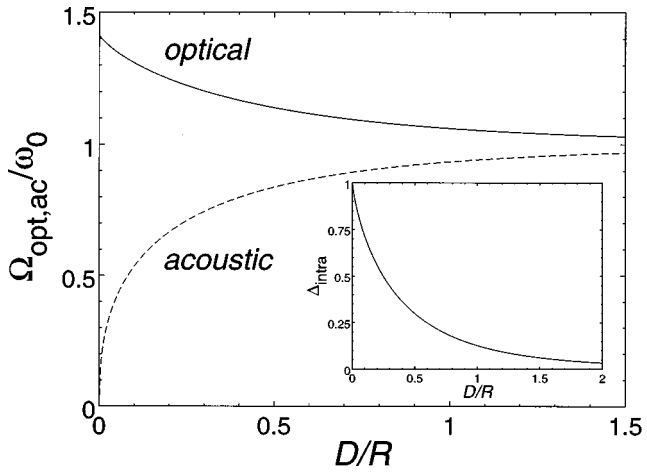

FIG. 2. Optical (solid) and acoustic (dashed) mode frequencies in a double-layered quantum-dot structure with identical parameters at $B=0$, as a function of the distance between layers. Intercell interaction is neglected. Inset shows the dependence of the intracell interaction parameter $\Delta_{\rm intra}$ on D/R.

as well as for other structures with two spatially separated plasma subsystems, such as, e.g., metal-dielectric-metal systems.[24]

The classical model used here (see also Ref. 12) does not describe correctly the behavior of the acoustic mode in the limit of the very small D. The quantum-mechanical calculations of Sec. III give the finite value of the acoustic mode frequency at $D \to 0$. This effect can be interpreted both quantum mechanically (see Sec. III) and classically (within the framework of the *nonlocal* hydrodynamic theory). In the hydrodynamic approach[25] the frequency of the 2D plasmons in a single layer is given by the formula

$$\omega^2(q) = \frac{2\pi n_s e^2}{m^\star \epsilon} q + s^2 q^2. \tag{23}$$

The first term in Eq. (23) is due to the Coulomb restoring force, the second one (neglected in our local classical theory) is due to the compressibility of the 2DES. The velocity s is defined by the relation $m^\star s^2 = \partial p/\partial n_s$, where p is a ''two-dimensional'' pressure, and for an ideal 2D Fermi gas equals $s = v_F/\sqrt{2}$. In a system of neutral particles ($e^2 = 0$) s would be the thermodynamic speed of sound. In a double-layered system an additional factor $2/[1 + \coth(qD/2)]$ arises in the first term in the spectrum of the acoustic mode. Due to this factor the first term vanishes in the limit of small D, i.e., the Coulomb restoring force disappears, while the last (compressibility) factor remains finite. In the double-layered dot structures the wave vector q is discretized, $q \simeq 1/R$, which leads to a finite frequency of the acoustic mode at $D \to 0$. Comparing two contributions to the spectrum of the acoustic mode one can see that the compressibility term can be neglected if $D \gg a_B/2$, where a_B is the effective Bohr radius. Our local classical approach thus correctly describes the optical mode at all D and the acoustic mode at $D > a_B$.

4. Linewidths

The damping of the $\pm$ polarized optical and acoustic modes (14) can be found from the dispersion equation (11) and is given by the expressions

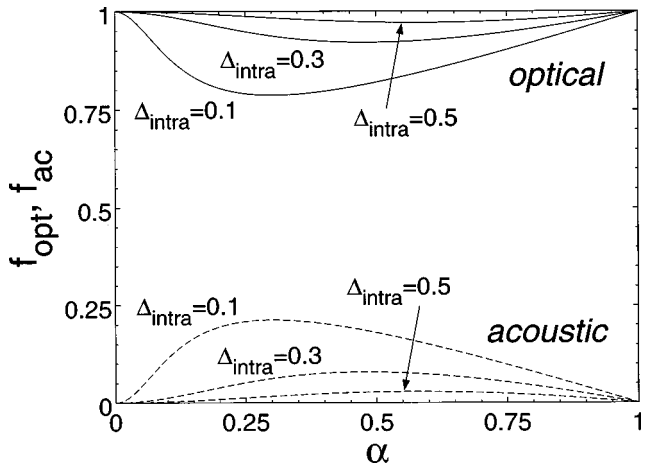

FIG. 3. Oscillator strengths of the optical (solid curves) and acoustic (dashed curves) modes at $B=0$ as a function of the density asymmetry parameter $\alpha \equiv (n_{s,1}-n_{s,2})/(n_{s,1}+n_{s,2})$ at different values of the intracell interaction Δ_{intra}.

$$\text{Im}\ \omega_{\pm}^{\text{opt,ac}} = -\frac{\gamma}{2}\left[1 \pm \frac{\omega_c/2}{\sqrt{(\omega_c/2)^2+\Omega_{\text{opt,ac}}^2}}\right]. \tag{24}$$

As in the case of single-layered dots, the damping of the + polarized optical and acoustic modes increases by a factor of 2 with increasing magnetic field, while the damping of the − polarized (edge-magnetoplasmon) modes decreases with increasing B.

In our quasistatic model we neglect the radiative effects that result in an additional contribution to the linewidth, Eq. (24). As has been shown in Ref. 19, the use of the full system of Maxwell equations instead of the Poisson equation (3) leads to the replacement of γ in Eq. (24) by $\gamma+\Gamma$, where Γ is the radiative decay of modes. The radiative effect is due to a coherent *dipole* radiation of plasma modes; for the *optical* mode in the double-layered quantum-dot structure the radiative decay Γ_{opt} is determined, similar to a single-layered case,[19] by the expression

$$\Gamma_{\text{opt}} = \frac{2\pi f(n_{s,1}+n_{s,2})e^2}{m^{\star}c\sqrt{\epsilon}}, \quad a \ll \lambda, \quad D \ll \lambda. \tag{25}$$

The radiative decay of the *acoustic* mode Γ_{ac} in a double-layered quantum-dot structure is much smaller, due to a smaller dipole moment of the acoustic mode, and vanishes in a symmetric structure.

5. Oscillator strengths

The oscillator strength of the acoustic mode is much smaller than that of the optical mode (see Fig. 1). Assuming again that the dots differ from each other only by the electron density we find from Eq. (10) at $B=0$,

$$f_{\text{opt,ac}} = \frac{1}{2}\left\{1 \pm \frac{\Delta_{\text{intra}}+\alpha^2(1-\Delta_{\text{intra}})}{[\Delta_{\text{intra}}^2+\alpha^2(1-\Delta_{\text{intra}}^2)]^{1/2}}\right\}; \tag{26}$$

the oscillator strengths f_{opt} and f_{ac} are normalized by the condition $f_{\text{opt}}+f_{\text{ac}}=1$. The dependence of f_{opt} and f_{ac} on the density asymmetry parameter $\alpha \equiv (n_{s,1}-n_{s,2})/(n_{s,1}+n_{s,2})$ at different values of Δ_{intra} is shown in Fig. 3. The oscillator strength of the acoustic mode vanishes at $\alpha=1$ (when there are no electrons in one of the dots) and at $\alpha=0$ (when the dots are identical). The acoustic mode has a maximum oscillator strength when

$$\alpha = \alpha_{\max} = \frac{\Delta_{\text{intra}}}{1+\Delta_{\text{intra}}}. \tag{27}$$

At $\alpha=\alpha_{\max}$ one has

$$f_{\text{opt,ac}}(\alpha_{\max}) = \frac{1}{2}\left[1 \pm \frac{2\Delta_{\text{intra}}^{1/2}}{1+\Delta_{\text{intra}}}\right].$$

The best conditions for experimental detection of the acoustic mode are thus determined by Eq. (27).

D. Discussion

Within our classical model we obtain an analytic description of the main features of the system: the absorption spectrum, the magnetic-field dependence of the excitation frequencies in systems with different physical and geometrical parameters, the influence of the intercell interaction on the excitation spectrum, and linewidths and oscillator strengths of the optical and acoustic modes. The classical model does not describe, however, effects conditioned by nonlocal and quantum corrections, which will be considered in the next section.

III. QUANTUM-MECHANICAL CALCULATION

A. Model

1. Main assumptions

In the quantum-mechanical model we calculate both the ground-state properties and the electromagnetic response of the system. We restrict ourselves to a single elementary cell of our periodic double-layered quantum-dot array, neglecting the intercell interaction. We assume that the dots have a circular symmetry and consider $\mathcal{N}$ mobile electrons in an external potential $V_{\text{ext}}(\mathbf{r},z) \equiv V_{\text{ext}}(r,z)$, $\mathbf{r}=(r,\varphi)$. We neglect the tunneling of electrons between dots in z direction, which implies that the distance D between dots exceeds the penetration length of the electron wave function under the barrier $\hbar/\sqrt{2m^{\star}V_B}$ (here V_B is the height of the barrier between dots). We neglect also the spatial spreading of the electronic wave functions in z direction by assuming a charge distribution according to Eq. (1). Thus we consider only Coulomb coupling between the layers. The Hartree and exchange-correlation electron-electron interaction are taken into account in the framework of the density-functional theory in the local-density approximation. Calculating the electromagnetic response in the RPA formalism we neglect the radiative effects. The sizes of the system and the distance between the dots are again assumed to be much smaller than the wavelength of light.

2. External potential

In a number of papers on single-layered quantum dots[14–18] the external potential has been modeled by a parabolic confinement $\sim a_2 r^2$ with some nonparabolic corrections ($\propto r^4$, r^6, etc). The coefficients of the expansion have been assumed to be independent external parameters of the

problem. For the *double-layered* quantum dot one has to make more accurate assumptions on the origin of the lateral, external potential. In principle, the external potential $V_{\rm ext}(\mathbf{r},z)$ is conditioned by a neutralizing background charge (positively charged ionized donors and negatively charged surface states), as well as by rectangular potential wells in the growth direction and the potential steps at the lateral boundaries due to the work function at the interface semiconductor vacuum. As electrons occupy only the planes $z=z_j$ (which means that the potential in growth direction is effectively taken into account), we need only to model the lateral confinement potential with a dependence on D. We assume that the background charge distribution in the system has the form

$$\rho^0_{\rm ext}(\mathbf{r},z)=\sum_{j=1}^{2}\left[\frac{e\mathcal{N}_j^+}{\pi R^2}\Theta(R-r)-\frac{e\mathcal{N}_j^-}{2\pi R}\delta(R-r)\right]\delta(z-z_j). \tag{28}$$

Thus, in our model the neutralizing background charge consists in two positively charged sheets with the radius R and the total number of positive charges $\mathcal{N}_j^+$, and two negatively charged ''guard'' rings with the radius R and the total number of negative charges $\mathcal{N}_j^-$ to model the surface states. We choose the number of mobile electrons in each dot to be $\mathcal{N}_j=\mathcal{N}_j^+-\mathcal{N}_j^-$ to achieve charge neutrality. In all calculations we assume that the number of surface charges is sufficiently large, so that the radius of the areas occupied by the mobile electrons R_e^j is smaller than the geometrical radius of the dots R. Under these conditions the potential steps at the lateral boundaries semiconductor vacuum do not influence the properties of the system. The external potential $V_{\rm ext}(\mathbf{r},z)$ is then determined by the Poisson equation with the background charge distribution given by Eq. (28).

In a recent work Steinebach, Heitmann, and Gudmundsson[13] have applied the density functional formalism, similar to that used in our paper, to a problem of double-layered quantum wires. They have assumed that the external potentials $V_{\rm ext}(\mathbf{r},z_j)$ are expanded in power series with *independent* coefficients. As seen however from the above discussion, the expansion coefficients in two layers *cannot be considered as independent quantities*: in real structures the curvature of the external potential in the middle of one layer obviously depends on the background charge density in the other layer, as well as on the interlayer distance D. As a result, the D dependence of the collective mode frequencies in Ref. 13 does not agree with the well-known results (e.g., the frequency of the optical mode does not depend on D), and contradicts the classical solution of the same problem given by Shikin, Demel, and Heitmann.[12]

3. Ground state

In order to calculate single-particle wave functions $\phi_\lambda^j(\mathbf{r})$, energy levels ϵ_λ^j and the ground-state density

$$n_j^0(\mathbf{r})=2\sum_\lambda f(\epsilon_\lambda^j)\,|\phi_\lambda^j(\mathbf{r})|^2 \tag{29}$$

we use the Kohn-Sham formalism of the density-functional theory. Here $f(\epsilon)$ is the Fermi distribution function, and the factor 2 takes into account the spin degeneracy of the states. Considering only the Coulomb coupling between the dots one can obtain a system of two coupled Kohn-Sham equations

$$\left[\hat{T}+V_{\rm ext}(\mathbf{r},z_j)+\sum_{k=1}^{2}\left[V_H^{jk}(\mathbf{r})+V_{\rm XC}^{jk}(\mathbf{r})\right]\right]\phi_\lambda^j(\mathbf{r}) =\epsilon_\lambda^j\phi_\lambda^j(\mathbf{r}),\quad j=1,2, \tag{30}$$

where $\hat{T}$ is the kinetic-energy operator which includes the vector potential in finite magnetic field B, and

$$V_H^{jk}(\mathbf{r})=\frac{e^2}{\epsilon}\int d\mathbf{r}'\,\frac{n_k^0(\mathbf{r}')}{\sqrt{|\mathbf{r}-\mathbf{r}'|^2+(z_j-z_k)^2}} \tag{31}$$

is the Hartree potential. The exchange-correlation potential $V_{\rm XC}^{jk}(\mathbf{r})$ is assumed to be diagonal in the layer indices, $V_{\rm XC}^{jk}=\delta_{jk}V_{XC}^j$, and is estimated in the local-density approximation,

$$V_{\rm XC}^j(\mathbf{r})=\frac{\delta}{\delta n_j^0}\int d\mathbf{r}'\,n_j^0(\mathbf{r}')\,\epsilon_{\rm XC}(n_j^0(\mathbf{r}')), \tag{32}$$

where $\epsilon_{\rm XC}$ is the exchange-correlation energy of the homogeneous 2DEG per electron,[26] and δ means the variational derivative.

To obtain a self-consistent solution of Eqs. (29)–(32) we use the circular symmetry of the problem and expand the Kohn-Sham orbitals $\phi_\lambda^j(\mathbf{r})=R_{nm}^j(r)e^{im\varphi}$ in the complete set of eigenfunctions of the two-dimensional harmonic oscillator with a curvature of the external potential in the centers of the dots. A numerical diagonalization provides the coefficients of the expansion. The procedure of calculating the ground state density, Eq. (29), and the total potential $V_{\rm ext}+V_H+V_{\rm XC}$ is done iteratively until self-consistency is achieved.

4. Electromagnetic response

The response of the system to an external uniform ac electric field $E_\alpha^{\rm ext}\propto\exp(-i\omega t)$ is described within the RPA formalism.[27] The charge density fluctuations in layers $\rho_j(\mathbf{r},\omega)$ satisfy the integral equation,

$$\sum_{k=1}^{2}\int d\mathbf{r}'\,\Xi_{jk}(\mathbf{r},\mathbf{r}',\omega)\rho_k(\mathbf{r}',\omega) =e^2\int d\mathbf{r}'\,\chi^j(\mathbf{r},\mathbf{r}',\omega)\Phi_{\rm ext}(\mathbf{r}',\omega), \tag{33}$$

where $\Phi_{\rm ext}(\mathbf{r},\omega)=-\mathbf{E}_\alpha^{\rm ext}\cdot\mathbf{r}$ is the potential of the external field, and $\chi^j(\mathbf{r},\mathbf{r}',\omega)$ is the susceptibility of a noninteracting electron gas,

$$\chi^j(\mathbf{r},\mathbf{r}',\omega)=\lim_{\Gamma\to0}2\sum_{\lambda\mu}\frac{f(\epsilon_\lambda^j)-f(\epsilon_\mu^j)}{\epsilon_\lambda^j-\epsilon_\mu^j+\hbar\omega+i\Gamma} \times\phi_\lambda^{j*}(\mathbf{r})\phi_\mu^j(\mathbf{r})\phi_\mu^{j*}(\mathbf{r}')\phi_\lambda^j(\mathbf{r}'). \tag{34}$$

The one-particle states $\phi_\lambda^j(\mathbf{r})$ and the one-particle energies ϵ_λ^j are taken from the solution of the Kohn-Sham system of Eqs. (29)–(32), and $\Xi_{jk}(\mathbf{r},\mathbf{r}',\omega)$ is a response function of the system,

$$\Xi_{jk}(\mathbf{r},\mathbf{r}',\omega)=\delta_{jk}\left[\delta(\mathbf{r}-\mathbf{r}')-\chi^{j}(\mathbf{r},\mathbf{r}',\omega)\frac{\delta V_{\mathrm{XC}}^{j}}{\delta n_{j}^{0}}\right]-\frac{e^{2}}{\epsilon}\int d\mathbf{r}''\frac{\chi^{j}(\mathbf{r},\mathbf{r}'',\omega)}{\sqrt{|\mathbf{r}'-\mathbf{r}''|^{2}+(z_{j}-z_{k})^{2}}}. \tag{35}$$

From the solution of the integral equation (33) we find the dipole moment

$$P_{\alpha}=\sum_{k=1}^{2}\int d\mathbf{r}x_{\alpha}\rho_{k}(\mathbf{r},\omega)\equiv\alpha_{\alpha\beta}(\omega)E_{\alpha}^{\mathrm{ext}} \tag{36}$$

and the polarizability of the whole system $\alpha_{\alpha\beta}(\omega)$. The absorption spectrum is then determined by the antihermitian part $(\alpha_{\alpha\beta}-\alpha_{\beta\alpha}^{\star})/2$ of the polarizability tensor.

To solve the integral equation (33) we expand the relevant quantities into Fourier series with respect to the angular coordinate φ. Thus, it reduces to a set of equations with different angular momentum quantum number l. In the uniform external ac electric field only the dipole modes with $l=\pm 1$ are excited. After discretization of the variable r we obtain instead of Eq. (33) a set of linear equations,

$$\hat{M}\vec{X}=\vec{C}, \tag{37}$$

where the matrix $\hat{M}$ comes from the kernel Ξ, $\vec{X}$ is the vector of the unknown charge-density fluctuation, and $\vec{C}$ is a known vector due to the right-hand side of Eq. (33). Then Eq. (37) is diagonalized numerically. The excitation spectrum of the system is determined by the equation

$$\det\hat{M}=0. \tag{38}$$

The RPA formalism,[27] which we use to calculate the FIR response of the system, generally yields good results in the high-density electron gas, $\pi n_s a_B^2>1$. Actually this approach has a wider region of applicability, at least in quantum dots. This is supported by the fact that our calculations for parabolic dots reproduce the statement of the generalized Kohn theorem,[28,22] which is exact in all orders of the parameter $(a_B\sqrt{n_s})^{-1}$. Below we use the RPA also at $\pi n_s a_B^2\lesssim 1$.

B. Results

1. Ground state

The calculated ground-state density and self-consistent potential at $B=0$ are shown in Fig. 4 for the following system. The number of positive charges in layers is $\mathcal{N}_1^+=220$, $\mathcal{N}_2^+=147$, the number of mobile electrons is $\mathcal{N}_1=60$, $\mathcal{N}_2=40$, so that $\mathcal{N}_j/\mathcal{N}_j^+$ is the same in both layers. The geometrical radius of the dots has been taken to be $R=100$ nm, and the distance $D=50$ nm. The solid curves on the potential plots show the external confining potential $V_{\mathrm{ext}}(r,z_j)$. The logarithmic divergency of the potential at the boundary of the system is due to the negatively charged ''guard'' rings. The dashed curves show the self-consistent potential calculated in the Hartree approximation. Including exchange-correlation terms results only in small changes of ground-state properties, but has no effect on the response properties for all systems considered here. The dotted curves show the parabolic part of the external potential.

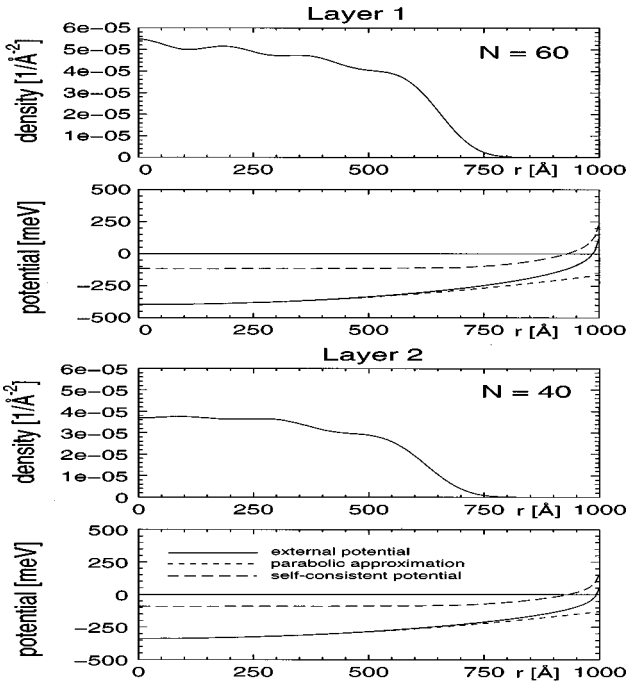

FIG. 4. The ground-state properties (density and self-consistent potential) for a system with $\mathcal{N}_1^+=220$, $\mathcal{N}_2^+=147$, $\mathcal{N}_1=60$, $\mathcal{N}_2=40$, $R=100$ nm, $D=50$ nm at $B=0$ ($\mathcal{N}_j/\mathcal{N}_j^+$ is the same in both layers).

2. Electromagnetic response

The absorption spectra obtained from the quantum-mechanical calculation do not essentially differ from those of Fig. 1(a). Additional features found in the magnetic-field dependence of the resonance frequencies are due to nonparabolicities in the lateral potential and non-local and quantum corrections neglected in the classical model. Calculations for dots with a relatively large number of electrons (Fig. 5) reveal the nonlocal Bernstein modes[29] at magnetic fields which occur at the intersection of both the optical and acoustic + polarized (upper) modes with the second harmonic of the cyclotron resonance $2\omega_c$. In a system with only few elec-

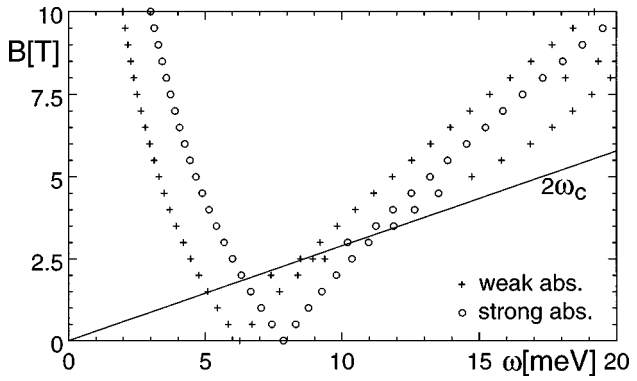

FIG. 5. Magnetic-field dependencies of the collective mode frequencies for a system with the same parameters as in Fig. 4. The $2\omega_c$ line is drawn to identify Bernstein modes.

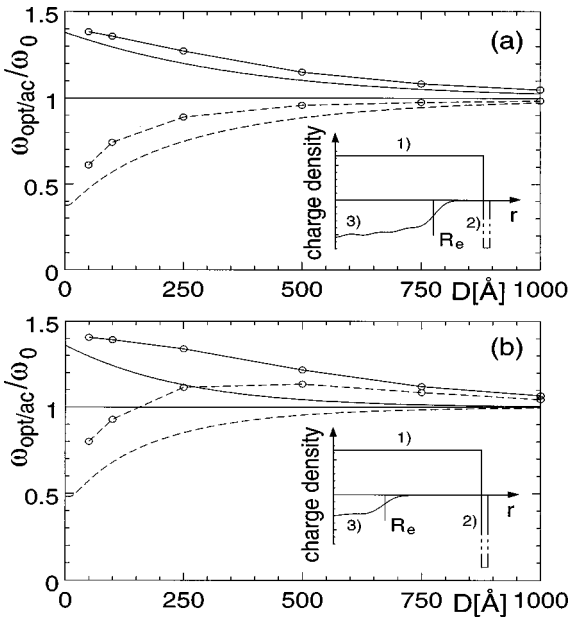

FIG. 6. Dependence of optical (solid line with circles) and acoustic (dashed line with circles) mode frequencies on the interlayer distance D for (a) $\mathcal{N}_1=\mathcal{N}_2=60$, $\mathcal{N}_1^+=\mathcal{N}_2^+=200$, $R=100$ nm ($R_e\approx 70$ nm); and (b) $\mathcal{N}_1=\mathcal{N}_2=10$, $\mathcal{N}_1^+=\mathcal{N}_2^+=200$, $R=100$ nm ($R_e\approx 40$ nm). Comparison is made with RPA results obtained for infinite 2DEG (see text). Insets show the distribution of equilibrium charge density with contributions of (1) positive background, (2) surface states, and (3) mobile electrons inside the dot.

trons per dot we have seen a splitting of both the optical and acoustic modes, similar to that found for quantum-dot helium in Ref. 30.

Figure 6 shows the D dependence of the optical- and acoustic-mode frequencies at $B=0$. The general behavior agrees with the results of the classical calculation and with the calculations for other double-layered systems:[12,24] as the Coulomb coupling increases for decreasing D, the frequency of the optical mode increases (by a factor of $\sqrt{2}$ at $D\rightarrow 0$), the frequency of the acoustic mode decreases [Fig. 6(a)]. However, one sees two additional features in the results of the quantum-mechanical calculation. First, in contrast to the classical result, the frequency of the acoustic mode does not tend to zero at $D\rightarrow 0$. The reason for this has been already discussed in Sec. II. From the quantum-mechanical point of view the finite value of the acoustic-mode frequency at $D=0$ is due to finite single-particle energy differences $\epsilon_\lambda^j-\epsilon_\mu^j$; see Eq. (34). This interpretation is supported by comparison with a RPA calculation for double-layered *infinite* 2DES. We take analytic formulas for the frequencies of the optical and acoustic modes of the double-layered infinite 2DES, $\omega_{\rm opt,ac}(q,D)$ (derived from the Poisson equation and the known Stern formula[31] for the polarizability of the 2DES), and replace the wave vector q of plasmons by $1/R_e$, where R_e is the calculated radius of the disk of mobile electrons [see insets in Figs. 6(a),(b)]. The resulting D dependencies $\omega_{\rm opt,ac}(R_e^{-1},D)$ are shown in Figs. 6(a),(b) by thin solid (optical) and dashed (acoustic mode) curves. A good agreement is found with the dot results, especially for dots with a large number of electrons [Fig. 6(a)]. The offset of the acoustic-mode frequency at $D\rightarrow 0$ in the 2DES is due to the Landau

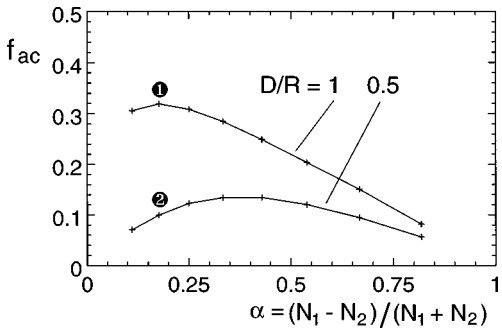

FIG. 7. Oscillator strengths of the acoustic mode from the quantum-mechanical model for $D/R=1$ and $D/R=0.5$. The parameters in the calculation are chosen under the condition that $\mathcal{N}_j/\mathcal{N}_j^+$ is the same in both layers ($\mathcal{N}_1=20$, $\mathcal{N}_1^+=200$, $\mathcal{N}_2=2,4,6,\ldots,16$, $\mathcal{N}_2^+=10\mathcal{N}_2$).

damping[32] at the edge of the continuum of single-particle states $\omega<qv_F+\hbar q^2/2m^\star$, $q=1/R_e$.

Another new feature which is seen in our quantum-mechanical calculation is a nonmonotonic behavior of the acoustic mode in a structure with small $\mathcal{N}$. This feature is seen neither in classical models nor in the quantum-mechanical RPA results for an infinite 2DES (with $q=1/R_e$). We believe that the reason for this behavior is a violation of the *local* charge neutrality in a small object like a quantum dot, which is taken into account in our full quantum-mechanical approach but is ignored in the simpler schemes. Indeed, both in the classical and in the quantum-mechanical RPA approach for an infinite 2DES, it is assumed that in equilibrium the system is locally neutral. The resonance frequencies are then determined by restoring forces that arise when the system deviates from the equilibrium. The D dependence of the resonance frequencies is only due to the D dependence of the Coulomb restoring force. In small objects, like double-layered quantum dots, there is no *local* charge neutrality in each dot even in equilibrium [see the equilibrium charge-density distributions in the insets of Figs. 6(a),(b). Therefore, the ground-state properties of the system (in particular, the single-particle energies ϵ_λ^j)] depend on D due to quadrupole and higher multipole interaction between the dots in equilibrium. As a result, the single-particle excitation spectrum is pushed up when D decreases, and due to this effect the collective modes $\omega_{\rm opt}$ and $\omega_{\rm ac}$ are also slightly pushed up as compared with models which assume the local charge neutrality. Consistent with this interpretation is the tendency found by comparing Figs. 6(a) and (b): the violation of local charge neutrality is stronger for the system with a smaller number of electrons and so is the deviation from the results from the infinite double-layered 2DEG.

Oscillator strengths of the optical and acoustic modes calculated in the quantum-mechanical model are shown in Fig. 7. They are in a good qualitative agreement with the results of the classical calculation (Fig. 3). A quantitative comparison of the classical and quantum-mechanical results is impossible as the radius of the mobile electron disk R_e depends on the density asymmetry parameter α in the quantum model.

A picture of charge-density fluctuations in the two layers (Fig. 8) allows us to illustrate the behavior of the oscillator strength of the acoustic mode. For larger D or weaker Cou-

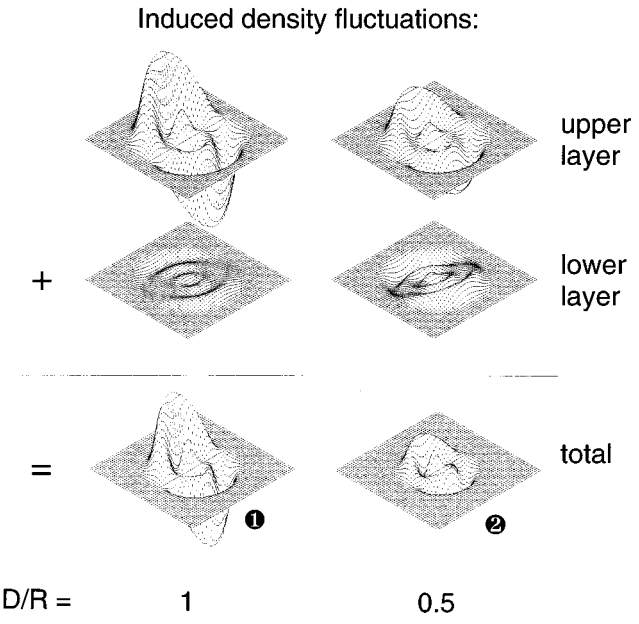

FIG. 8. Patterns of the induced charge density fluctuations for the acoustic mode, corresponding to the data points indicated in Fig. 7 ($\mathcal{N}_1=20$, $\mathcal{N}_1^+=200$, $\mathcal{N}_2=14$, $\mathcal{N}_2^+=140$).

lomb coupling (left panel of Fig. 8) the excitation is stronger localized in the upper layer (whose eigenfrequency is closer to the acoustic mode frequency) than for smaller D (right panel). As a consequence the compensation of induced charge density due to out-of-phase motion in upper and lower layer is less efficient (e.g., the induced dipole moment and thus the oscillator strength is larger) for larger D. In the case of a larger distance D, also the positions of the maxima of the induced density fluctuations deviate stronger from the values of $\Delta\varphi=0$ and 180° for the optical and acoustic mode, respectively, which also gives a contribution to this effect. Thus, beside in a splitting of the collective excitations into optical and acoustic modes, the Coulomb coupling between the layers results also in a stronger participation in the excitation of the otherwise less affected layer in each case.

IV. CONCLUSION

By applying classical and quantum-mechanical concepts we have studied the spectrum of collective excitations in double-layered quantum dots. It consists of two modes, the optical mode and the acoustic mode, which correspond to in-phase and out-of-phase oscillations of the electron density in the layers, respectively. The B dispersion of the modes, Eq. (14), is quite similar to those in a single quantum dot. The dependence of the optical- and acoustic-mode frequencies on the interlayer distance D is due to the interdot Coulomb coupling. The quantum-mechanical results (Figs. 5 and 6) differ from the classical ones (Figs. 1 and 2) by (i) showing the Bernstein modes (due to nonlocal effects), (ii) by the nonmonotonic behavior of the acoustic-mode frequencies versus D, which can be ascribed to the violation of the local charge neutrality in our microscopic dot model, and (iii) a nonvanishing acoustic-mode frequency for $D\rightarrow 0$. The oscillator strength of the acoustic mode (Figs. 3 and 7) is always smaller than that of the optical mode and vanishes in the limit of identical dots. We have derived an optimum condition for the observation of the acoustic mode (27).

An additional mode found in FIR experiments[10] has been interpreted as an acoustic mode observable due to a slight asymmetry in the electron density in a double-layered dot system (the values $n_{s,1}=7.7\times10^{11}$ cm^{-2}, $n_{s,2}=7.0\times10^{11}$ cm^{-2} have been determined from the Landau-level filling factor dependent periodic oscillations of the frequency of the $\omega_-^{\rm opt}$ mode). The intensity of this mode was about 10% of the optical mode. As follows, however, from our results, Eq. (26), Figs. 3 and 7, the oscillator strength of the acoustic mode would be practically negligible under the experimental conditions ($\alpha\approx0.046$, $\Delta_{\rm intra}\approx0.4$). We believe, therefore, that the mode observed in Ref. 10 is *not* the acoustic plasma mode and should be due to another reason.

The electron effective mass which can be extracted from experimental data of Ref. 10 for the optical mode, give the value $m^*=0.085m_0$, which is larger than the effective mass of 3D electrons at the bottom of the conduction band in GaAs $m^*=0.067m_0$ due to the quantum-size effect and the nonparabolicity of the GaAs conduction band. It is interesting that the experimental points identified in Ref. 10 as the acoustic mode fit ideally to a line $\omega=eB/m^*c$ with $m^*=0.067m_0$. This would correspond to the cyclotron resonance of 3D electrons of the GaAs substrate.

To conclude, we have calculated the ground-state properties, the FIR absorption and excitation spectra of a square lattice of double-layered quantum dots. We have discussed the dependencies of the observable values, intercell and intracell interactions in the system, collisional and radiative dampings of the optical and acoustic modes, influence of the electroneutrality of the system on the excitation spectrum. We have calculated the oscillator strengths of the optical and acoustic modes and found the conditions of the best observation of the acoustic mode.

ACKNOWLEDGMENTS

This work was supported by the Deutsche Forschungsgemeinschaft (SFB 348) and the NATO Science Program. One of us (S.M.) acknowledges the support of the Alexander von Humboldt Foundation. We thank the authors of Ref. 13 for communicating their results prior to publication.

*Present address: Max-Planck-Institut für Physik komplexer Systeme, Nöthnitzer Str. 38, D-01187 Dresden, Germany.

[1] For a review of early work on 2D plasmons see T. N. Theis, Surf. Sci. **98**, 515 (1980).

[2] D. Heitmann, Surf. Sci. **170**, 332 (1986).

[3] A. V. Chaplik, Superlattices Microstruct. **6**, 329 (1989).

[4] For a review see, e.g., D. Heitmann and J. P. Kotthaus, Phys. Today **46** (6), 56 (1993).

[5] A. Pinczuk, M. G. Lamont, and A. C. Gossard, Phys. Rev. Lett. **56**, 2092 (1986).

[6] G. Fasol, N. Mestres, H. P. Hughes, A. Fischer, and K. Ploog, Phys. Rev. Lett. **56**, 2517 (1986).
[7] T. Demel, D. Heitmann, P. Grambow, and K. Ploog, Appl. Phys. Lett. **53**, 2176 (1988).
[8] T. Demel, D. Heitmann, P. Grambow, and K. Ploog, Phys. Rev. B **38**, 12 732 (1988).
[9] T. Demel, D. Heitmann, P. Grambow, and K. Ploog, Superlattices Microstruct. **5**, 287 (1989).
[10] K. Bollweg, T. Kurth, D. Heitmann, V. Gudmundsson, E. Vasiliadou, P. Grambow, and K. Eberl, Phys. Rev. Lett. **76**, 2774 (1996).
[11] S. Katayama, J. Phys. Soc. Jpn. **60**, 1123 (1991).
[12] V. Shikin, T. Demel, and D. Heitmann, Phys. Rev. B **46**, 3971 (1992).
[13] C. Steinebach, D. Heitmann, and V. Gudmundsson, Phys. Rev. B **56**, 6742 (1997).
[14] D. A. Broido, K. Kempa, and P. Bakshi, Phys. Rev. B **42**, 11 400 (1990).
[15] V. Gudmundsson and R. R. Gerhardts, Phys. Rev. B **43**, 12 098 (1991).
[16] V. Gudmundsson, A. Brataas, P. Grambow, B. Meurer, T. Kurth, and D. Heitmann, Phys. Rev. B **51**, 17 744 (1995).
[17] T. Darnhofer, U. Rössler, and D. A. Broido, Phys. Rev. B **52**, R14 376 (1995).
[18] T. Darnhofer, U. Rössler, and D. A. Broido, Phys. Rev. B **53**, 13 631 (1996).
[19] S. A. Mikhailov, Phys. Rev. B **54**, 10 335 (1996).
[20] S. J. Allen, Jr., H. L. Störmer, and J. C. M. Hwang, Phys. Rev. B **28**, 4875 (1983).
[21] R. P. Leavitt and J. W. Little, Phys. Rev. B **34**, 2450 (1986).
[22] P. Bakshi, D. A. Broido, and K. Kempa, Phys. Rev. B **42**, 7416 (1990).
[23] C. Dahl, J. P. Kotthaus, H. Nickel, and W. Schlapp, Phys. Rev. B **46**, 15 590 (1992).
[24] See, e.g., a number of review articles in *Surface Polaritons: Electromagnetic Waves at Surfaces and Interfaces*, edited by V. M. Agranovich and D. L. Mills (North-Holland, Amsterdam, 1982).
[25] A. L. Fetter, Ann. Phys. (N.Y.) **81**, 367 (1973).
[26] M. Jonson, J. Phys. C **9**, 3055 (1976).
[27] See, e.g., A. Zangwill and P. Soven Phys. Rev. A **21**, 1561 (1980), and references therein.
[28] L. Brey, N. F. Johnson, and B. I. Halperin, Phys. Rev. B **40**, 10 647 (1989); P. A. Maksym and T. Chakraborty, Phys. Rev. Lett. **65**, 108 (1990).
[29] I. B. Bernstein, Phys. Rev. **109**, 10 (1958).
[30] D. Pfannkuche and R. Gerhardts, Phys. Rev. B **44**, 13 132 (1991).
[31] F. Stern, Phys. Rev. Lett. **18**, 546 (1967).
[32] In the double-layered quantum-dot structure with a completely discrete energy spectrum the Landau damping does not contribute to the linewidth of excitations as the frequencies of single-particle transitions [poles of the response function Ξ, Eq. (35)] never coincide with the frequencies of collective modes (zeros of Ξ).